

AD 668161

USNRDL-TR-68-28
15 January 1968

ELECTROCHEMICAL CORROSION STUDIES OF GALVANICALLY COUPLED SNAP-21 MATERIALS

by

D. A. Kubose
H. I. Cordova

**U.S. NAVAL RADIOLOGICAL
DEFENSE LABORATORY**

SAN FRANCISCO • CALIFORNIA • 94135

This document has been approved
for public release and sale; its
distribution is unlimited.

DDC
REF ID: A668161
APR 29 1968
SUITE
C

NUCLEAR APPLICATIONS BRANCH
D. L. Love, Head

NUCLEAR TECHNOLOGY DIVISION
R. Cole, Head

ADMINISTRATIVE INFORMATION

The work reported is part of a project sponsored by the Atomic Energy Commission, DRD&T Program, under AT-RDT-XP-141, Tasks 2a and 3b.

DDC AVAILABILITY NOTICE

This document has been approved for public release and sale; its distribution is unlimited.

ADDITION OF	
DDC	WRITE SECTION <input checked="" type="checkbox"/>
UNANNOUNCED	DIFF SECTION <input type="checkbox"/>
JUSTIFICATION	<input type="checkbox"/>
BY	
DISTRIBUTION/AVAILABILITY CODES	
DIST.	AVAIL. and or SPECIAL
1	

Eugene P. Cooper
Eugene P. Cooper
Technical Director

D C Campbell
D C Campbell, CAPT USN
Commanding Officer and Director

ABSTRACT

Electrochemical corrosion rate measurements on materials used in the SNAP-21 radioisotopically-fueled power system have been made in seawater at room temperature. The materials examined included aluminum, copper, Hastelloy C, Hastelloy X, nickel, 304 stainless steel, tantalum, titanium-621 alloy and uranium-8 % molybdenum alloy. The normal corrosion rate of each material was measured by means of galvanostatic polarization techniques. A galvanic series of the materials in seawater was determined and the galvanic currents between galvanically coupled materials were measured with a zero-resistance ammeter circuit. The effect of galvanic coupling of construction materials of the SNAP-21 system does not materially change the containment time of the Sr-90 fuel in the corrosive seawater environment.

SUMMARY

The Problem

Radiological-safety consideration of the SNAP-21 radioisotopically-fueled power system (for marine environment use) requires that the corrosion behavior in seawater of the various materials used in the interior construction of the system be known in the event that the pressure vessel, made of titanium 621 alloy, is breached. Materials used in the interior of the system include: aluminum, copper, Hastelloy C, Hastelloy X, nickel, 304 stainless steel, tantalum, and uranium-8 % molybdenum alloy. Knowledge of the seawater corrosion behavior of these materials individually and galvanically coupled will permit estimates of how long the radioactive fuel would be contained in the event that seawater entered the interior of the SNAP-21 system.

The Findings

Experiments were conducted to determine (1) the normal (i.e., uncoupled) corrosion rate of each material in seawater, (2) a galvanic series of the materials in seawater and (3) the effect on the corrosion rate of galvanically coupling the materials in seawater. The results of these experiments indicated that if seawater entered the interior of the SNAP-21 system, the radiological hazard to man would not constitute a serious threat, since the fuel would remain contained for a relatively long period of time.

It is felt that studies such as those carried out here would be of value in evaluating other radioisotopically-fueled SNAP systems in the Navy's SNAP program from the standpoint of radiological safety.

I. INTRODUCTION

The SNAP-21 system has been designed and is presently being developed by the Minnesota Mining and Manufacturing Company (3M) under the sponsorship of the Division of Reactor Development and Technology of the United States Atomic Energy Commission. The system is a radioisotopically-fueled power source providing 10 watts of electrical energy through thermoelectric conversion of the radioisotopically generated heat energy.

The radioisotopic nature of the fuel material, strontium-90 titanate, dictates that utmost precautions be taken to insure that man will not be subjected to its radiological hazards under credible accident situations.

Under normal deployment conditions the outside pressure vessel, made of titanium 621, is the only part of the system exposed to the ocean environment. It is possible, however, that seawater may enter the interior of the system in the event of a severe accident situation. Since there are a variety of metallic materials used in the interior of the SNAP-21 system, the presence of seawater can establish galvanic cells between them. This situation can lead to accelerated corrosion of these materials.

Because of these considerations it is necessary to examine the corrosion behavior of the materials comprising the SNAP-21 system resulting from exposure to seawater.

This report describes studies, using electrochemical techniques, to determine the corrosion behavior of the various materials used in the construction of the SNAP-21 system. These materials include aluminum, copper, Hastelloy C, Hastelloy X, nickel, 304 stainless steel, tantalum, titanium 621 alloy and uranium-8 % molybdenum alloy.

Three types of results are presented: (1) the normal (i.e., uncoupled) corrosion rate of each material; (2) a galvanic series of the materials; and (3) the effect of galvanically coupling the materials. From the integration of these results an attempt was made to estimate how long the radioisotopic fuel would be contained.

II. EXPERIMENTAL

The test specimens of the SNAP-21 materials were fabricated at NRL into electrodes from bar stock provided by 3M. The test electrodes were fabricated in the shape of right circular cylinders 0.5 in. in height and 0.25 in. in diameter (the U-8 % Mo electrode, fabricated from larger bar stock, was larger: 0.5 in. in height and 0.5 in. in diameter). Each electrode had a 4-40 threaded stud extending from one end for mounting on the electrode holder assembly of the polarization apparatus. Before use, each electrode was polished (finishing with 600 grit) and then ultrasonically cleaned in benzene and absolute ethanol. Immediately before immersion in the test seawater the electrodes were rinsed with distilled water.

The seawater used for the corrosion tests was collected about a mile from the Farallon Islands, located about 20 miles off the northern California coast at San Francisco. Before use the seawater was filtered through a Millipore filter (0.8 micron).

Conditions of aeration and deaeration of the seawater were achieved by continuous purging with air or nitrogen. All measurements were conducted at ambient room temperature (ca. 23°C).

Measurement of Normal Corrosion Rates

The normal corrosion rate of each of the SNAP-21 materials was determined by use of the galvanostatic polarization technique. The theory behind the application of the techniques has been adequately described in the literature.* A description of the polarization equipment and the experimental techniques used in this work has been given elsewhere.¹

In essence the galvanostatic technique is to cathodically and anodically polarize the test electrode from its open-circuit potential by application of an external current. The degree of polarization, measured as overvoltage E , is plotted against the logarithm of the applied current density, i . For values of E greater than about 50 mv such a plot should yield a straight line with slope β_c for cathodic polarization and β_a for anodic polarization. Values of the corrosion current density, i_{corr} , can be obtained from such measurements in two ways. One consists of applying the relation^{2,3}

*See for example M. G. Fontana and N. D. Greene, Corrosion Engineering. New York, McGraw Hill Book Company, 1967, Chapters 9 and 10.

$$\frac{\Delta E}{\Delta i} = \frac{\beta_a \beta_c}{i_{\text{corr}} (2.3) (\beta_a + \beta_c)} \quad (1)$$

where $\Delta E/\Delta i$ is the slope near the region of the open-circuit potential (i.e., E less than about 50 mv) for which the change of E with i is linear. The other method of obtaining i_{corr} is the extrapolation of the line of slope β_c to the open-circuit potential. The current density at the intersection represents the dissolution rate of the electrode and hence its corrosion rate in terms of current density.

Determination of Galvanic Series and of Effect of Galvanic Coupling (Currents)

The open-circuit potential of each test electrode was measured with respect to a saturated calomel reference electrode (SCE) in aerated and in deaerated seawater. All of the test electrodes were immersed in a common container while the measurements were made. These potentials were the basis for determining a galvanic series of the SNAP 21 materials.

The galvanic currents between each of the materials in turn and all the others, as a group, when short-circuited (i.e., galvanically coupled) to each other, were measured, in aerated and deaerated seawater, in the following manner. After the open-circuit potentials were determined, all but one, say Hastelloy X, of the test electrodes were short-circuited to each other. The connection between the shorted group of electrodes and Hastelloy X was made via a zero resistance ammeter circuit (ZRA) described by Greene.⁴ Now, in effect, all of the other electrodes were shorted to each other so that the galvanic current between Hastelloy X and the shorted group of electrodes could be measured. After measurement of this galvanic current, the ZRA was disconnected from the Hastelloy X, the Hastelloy X shorted (now directly) to the shorted group of electrodes, and a different electrode disconnected from the shorted group (which now included Hastelloy X) and re-connected to the shorted group via the ZRA. The galvanic current between this new single electrode and the new shorted group was measured. This procedure was followed until the galvanic current between each electrode and the shorted group had been measured (the shorted group being different for each measurement); these currents were denoted as the first set. Examination of this first set of galvanic currents revealed, by their direction, which electrode (or electrodes) was the anode in reference to the other electrodes. This electrode (or electrodes) was disconnected entirely and the above procedure repeated to obtain a second set of galvanic currents. This second set revealed another anodic electrode(s). It was disconnected entirely (so that now two electrodes had been removed) and the entire procedure repeated again to obtain a third set of galvanic currents. This procedure was followed until only two electrodes

remained, the galvanic current (the last set) between them also being measured by the ZRA. This technique, in addition to providing the galvanic currents, provides an independent determination of the galvanic series. The anodic electrode in the first set of galvanic currents is the most active and the remaining electrode after the last set is the most noble.

Determination of Polarization Behavior (Potentials)

The polarization behavior (see discussion in Section III) of the various anodic and cathodic members of the galvanic couples was determined in the following manner with a new set of test electrodes. After the open-circuit potential of each test electrode was individually measured (against the SCE), all but the test electrode with the most negative potential (the anode: most active in the galvanic series) were shorted together. The potential of this shorted group (the cathode) was measured against the SCE; then the anode and cathode were shorted to each other and the potential of the resulting couple measured against the SCE. After these potential measurements were completed the electrode which was the anode was disconnected and put aside. Another electrode, the one next most negative in potential, was disconnected from the shorted group and became the new anode (the shorted group, minus this electrode, became the new cathode). The above set of potential measurements was recorded in the same sequence with this new set of anode, cathode and couple. (The couple for this set was of course the cathode for the previous set. However cathode and couple readings were repeated for each set.) This procedure was repeated until only two electrodes remained, the cathodic one being the most noble* in the galvanic series and the anodic one being the next most noble. Comparison of the potentials of the various cathodes (consisting of the various shorted groups of electrodes) and anodes with their respective coupled potentials permitted evaluation of their respective polarization behavior.

In both the normal and the galvanic corrosion rate determinations the electrochemical equivalents of the corrosion rate, i.e., the corrosion current and the galvanic current in terms of current density ($\mu\text{ amp/cm}^2$), were measured. Faraday's Law was then used to translate these values of current density into a more immediately useful quantity such as mil per year (mpy). In application of Faraday's Law the following valencies were assumed for the corrosion products in seawater: +2 for nickel, copper, 304 stainless steel, Hastelloy C and Hastelloy X; +3 for Al; +4 for titanium 621 and Uranium-8 % molybdenum, +5 for tantalum. The relationship between current density in $\mu\text{amp/cm}^2$ and corrosion rate in mpy is

$$\text{Corrosion rate, mpy} = 0.129 \left(\frac{\text{eq.wt., g/g.eq.}}{\text{density, g/cm}^3} \right) \left(\text{current density, } \mu\text{amp/cm}^2 \right) \quad (2)$$

where the equivalent weight (g) and density (g/cm^3) refer to the electrode material.

*This turned out to be Hastelloy X, for both aerated and deaerated seawater.

III. RESULTS AND DISCUSSION

Normal Corrosion Rates

Figures 1 through 8 show some representative plots of E vs. $\log i$ from which values of β_a and β_c were obtained. In some instances the determination of β_a and β_c was somewhat subjective. However, this subjectivity does not affect the value of i_{corr} too severely since the term $\beta_a\beta_c/(\beta_a+\beta_c)$ in eq. (1) is relatively insensitive to small changes in β_a or β_c . Figures 9 through 12 show some representative plots of E against i in the region near the open-circuit potential. Values of $\Delta E/\Delta i$ were obtained from these plots.

Table 1 summarizes the electrochemical data and presents the corrosion currents in $\mu\text{amp}/\text{cm}^2$ and the normal corrosion rates in mpy for each of the SNAP-21 materials. The main table entries for i_{corr} and normal corrosion rate are based on Equation 1; the corresponding entries in parentheses are obtained by graphical extrapolation of β_c to the open-circuit potential.

Galvanic Series and Galvanic Effect

Figures 13 and 14 show the open-circuit potentials of the SNAP-21 materials as a function of time in aerated and deaerated seawater, respectively. The important features to note in these figures are not the values of the individual potentials but rather the relative positions of the materials with respect to one another. Also note that after a few hours, the potentials for the aerated seawater materials are relatively constant, whereas for the deaerated seawater materials changes are still occurring up to 100 hours. Because of this fact it is difficult to determine a galvanic series accurately. Nevertheless, Figs. 13 and 14 indicate, in general, what the galvanic series are. The most negative potential is shown by the most active material (i.e., the material on which accelerated corrosion takes place when it is coupled with materials more positive in potential) and the most positive potential is shown by the most noble material (i.e., the material which tends to be protected from corrosion when coupled to materials more negative in potential).

Tables 2 and 3 show the various sets (rows) of galvanic current densities measured between one material at a time and all the other coupled materials (in that row) in aerated and deaerated seawater, respectively. These current densities are obtained from the zero resistance ammeter measurements. The anodic member(s) of each set is denoted by its underlined galvanic current density. These anodic current densities are a measure

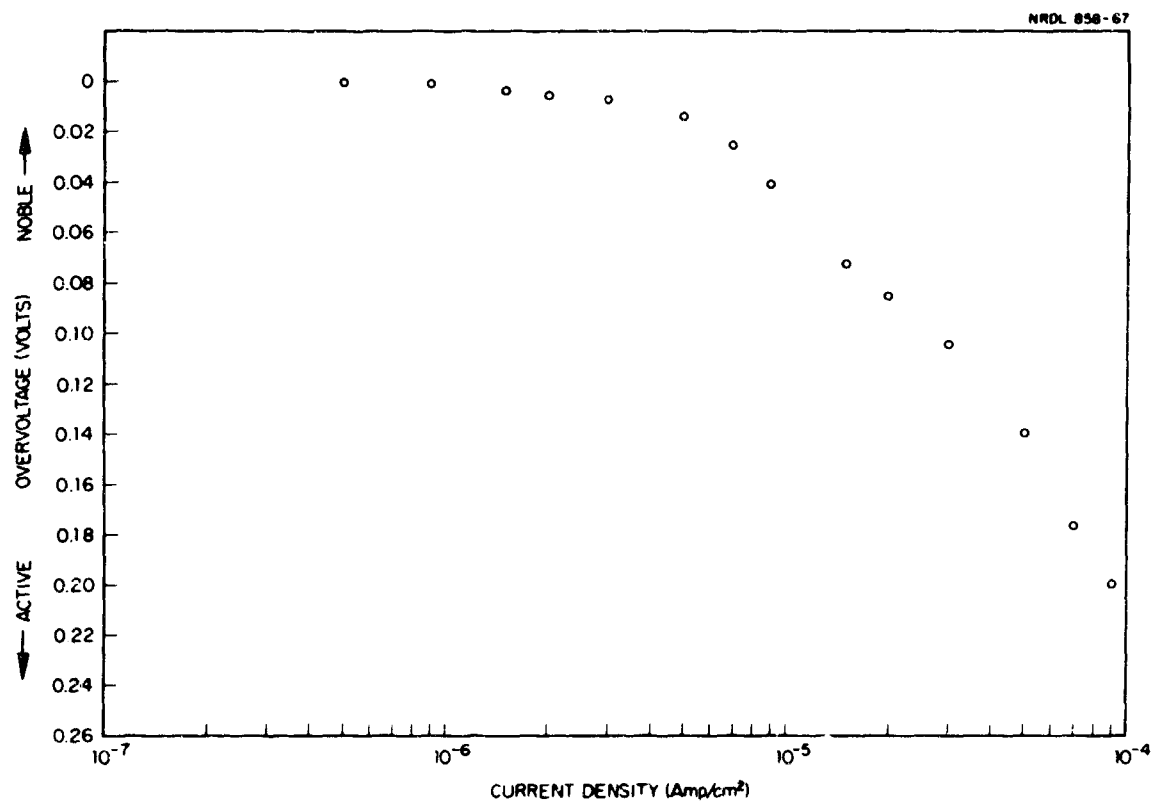


Fig. 1 Galvanostatic Cathodic Polarization of Copper in Aerated Seawater.

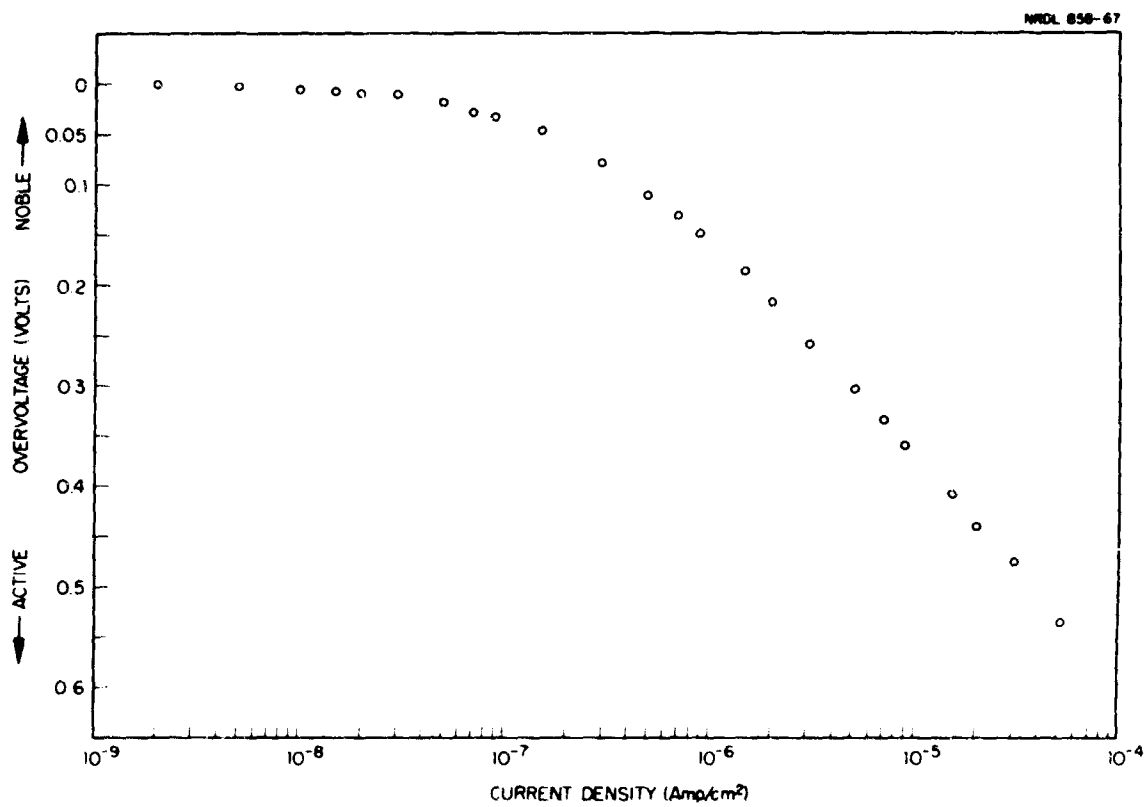


Fig. 2 Galvanostatic Cathodic Polarization of Aluminum in Aerated Seawater.

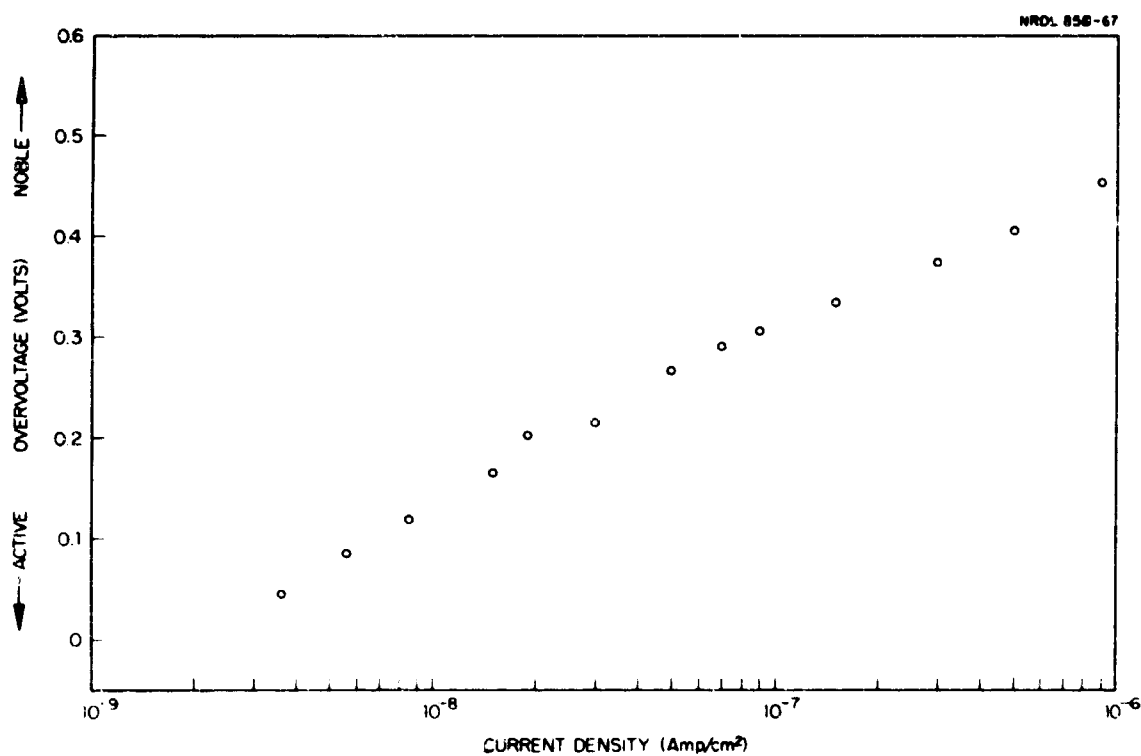


Fig. 3 Galvanostatic Anodic Polarization of Hastelloy X in Aerated Seawater.

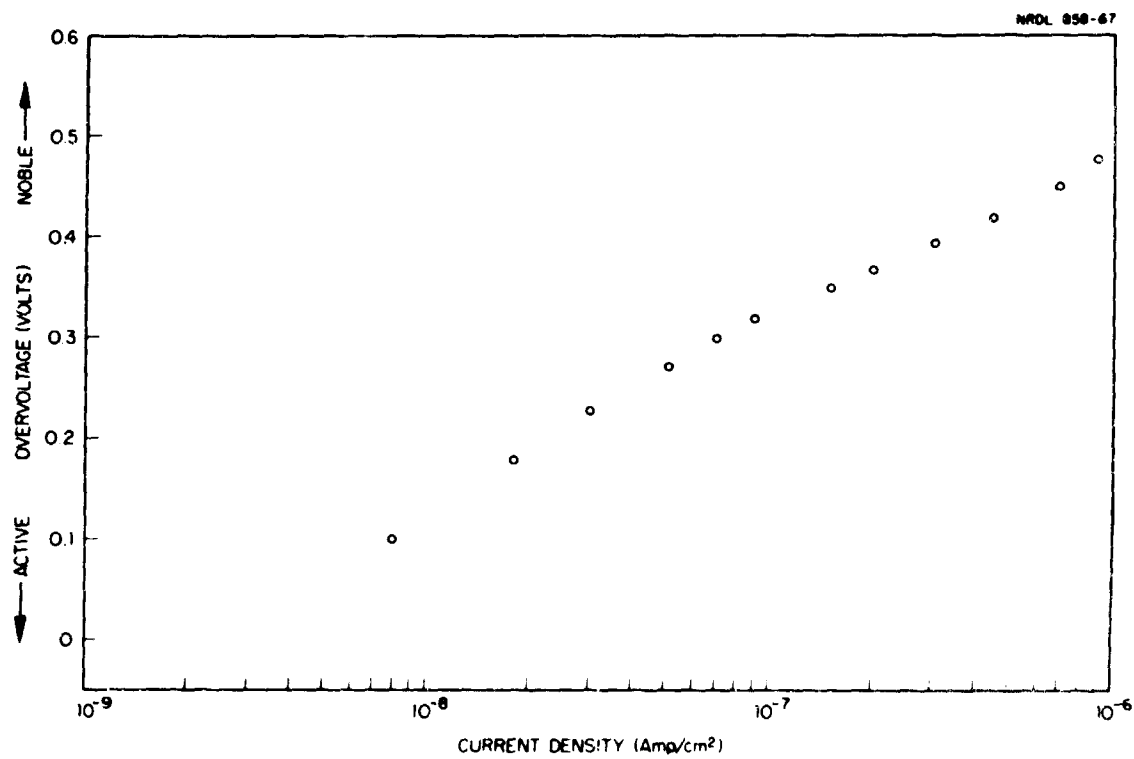


Fig. 4 Galvanostatic Anodic Polarization of Titanium-621 Alloy in Aerated Seawater.

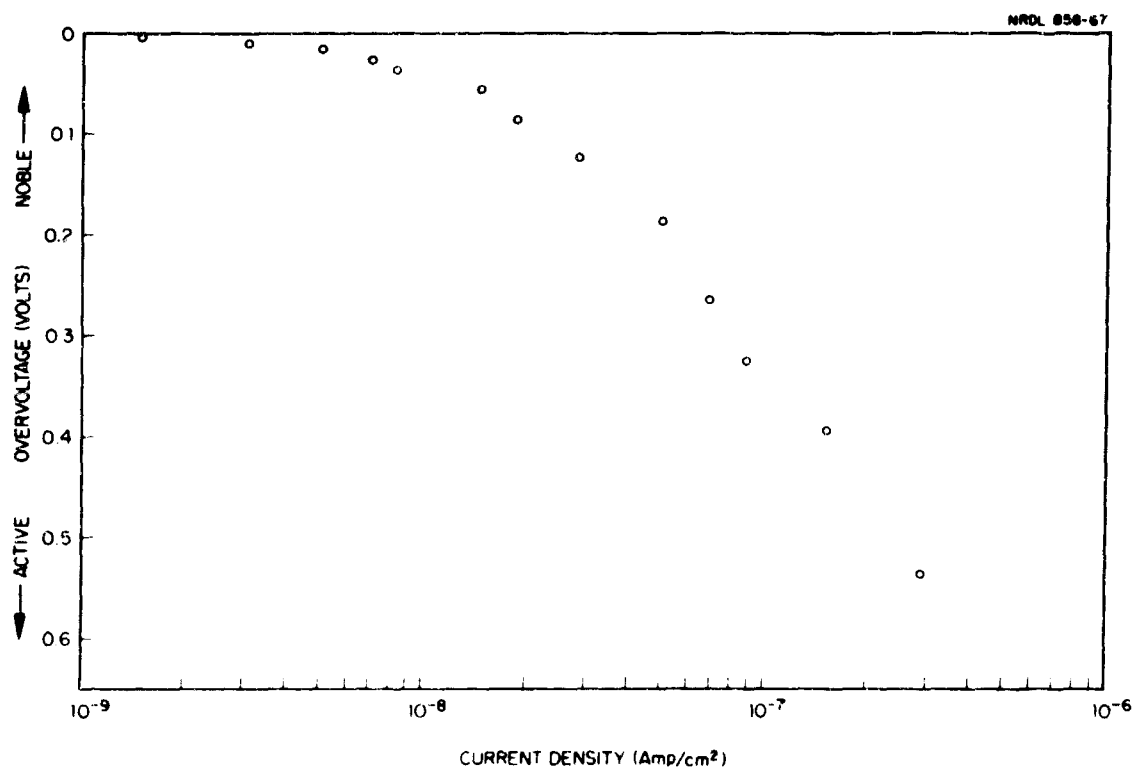


Fig. 5 Galvanostatic Cathodic Polarization of Tantalum in Deaerated Seawater.

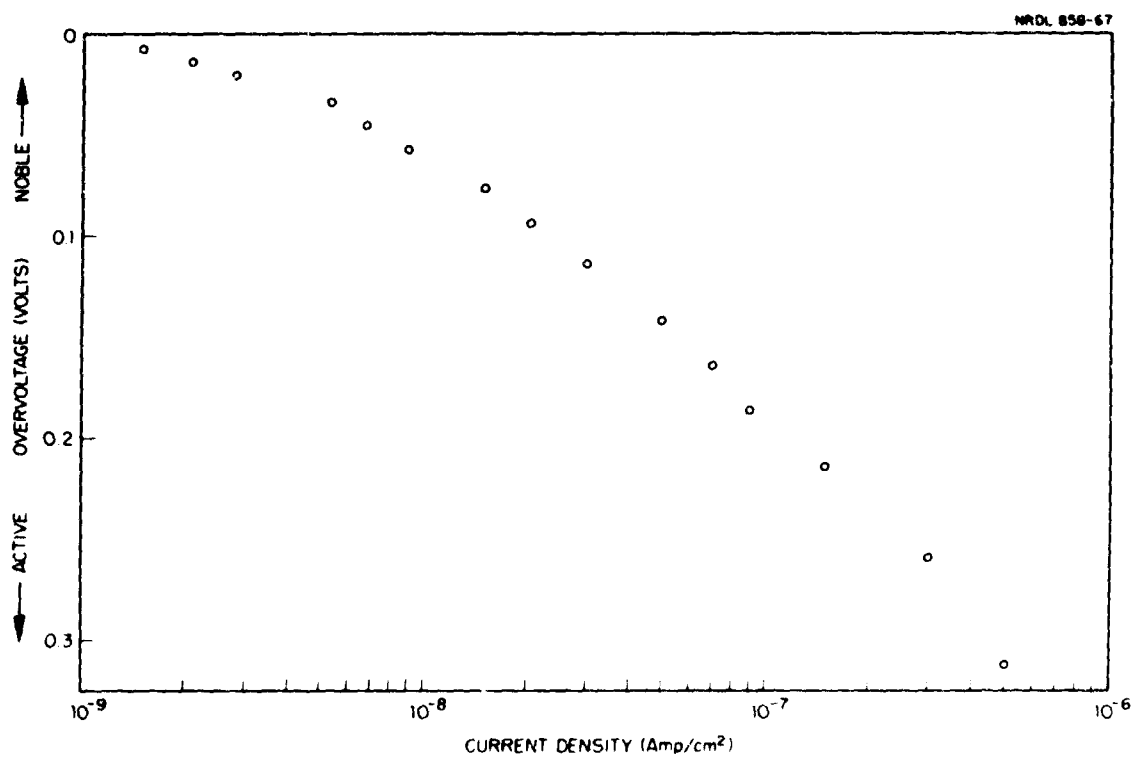


Fig. 6 Galvanostatic Cathodic Polarization of Nickel in Deaerated Seawater.

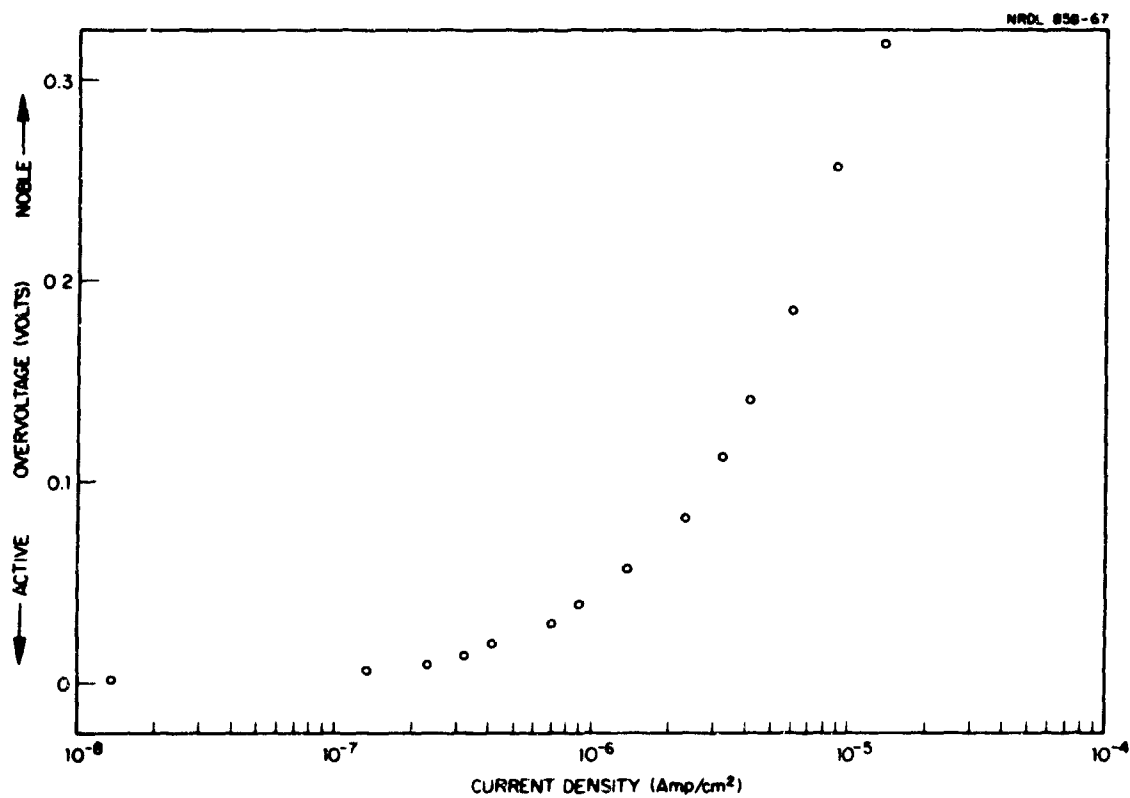


Fig. 7 Galvanostatic Anodic Polarization of Uranium-8 % Molybdenum Alloy in Deaerated Seawater.

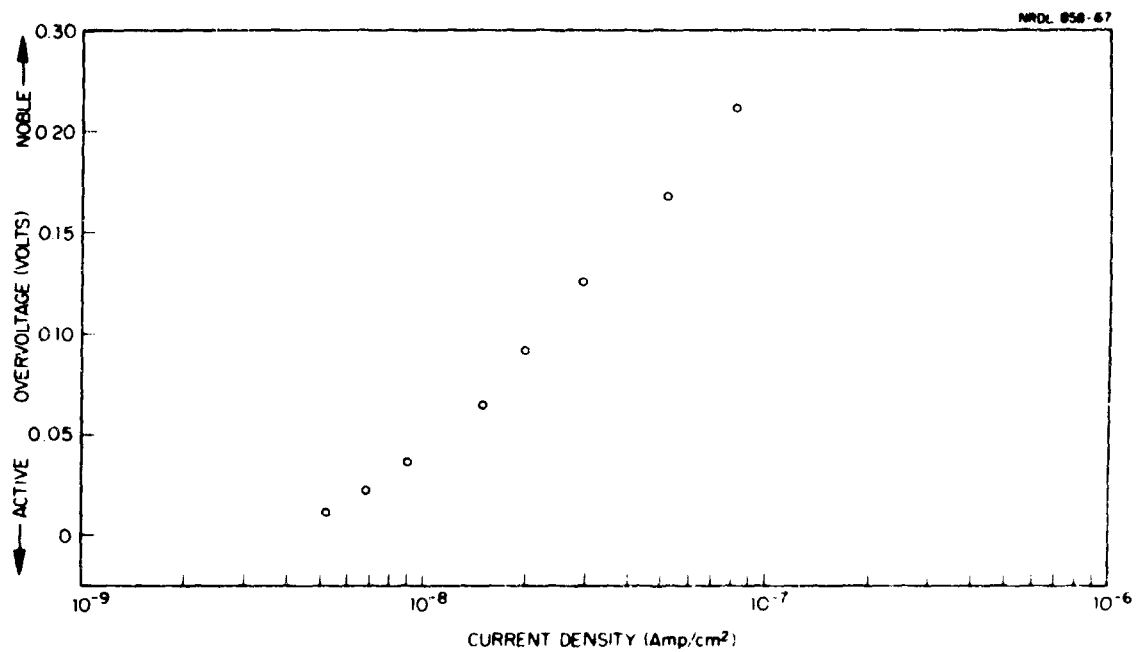


Fig. 8 Galvanostatic Anodic Polarization of 304 Stainless Steel in Deaerated Seawater.

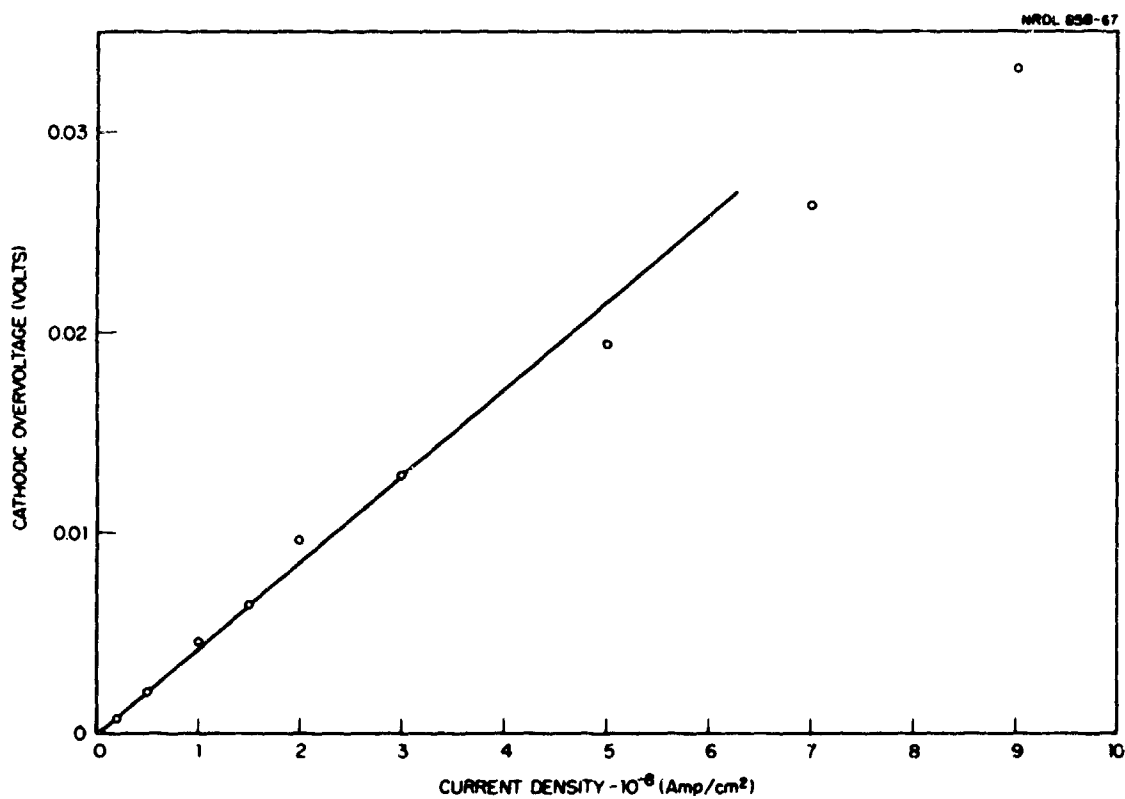


Fig. 9 Linear Plot of Cathodic Overvoltage vs. Current Density for Aluminum in Aerated Seawater.

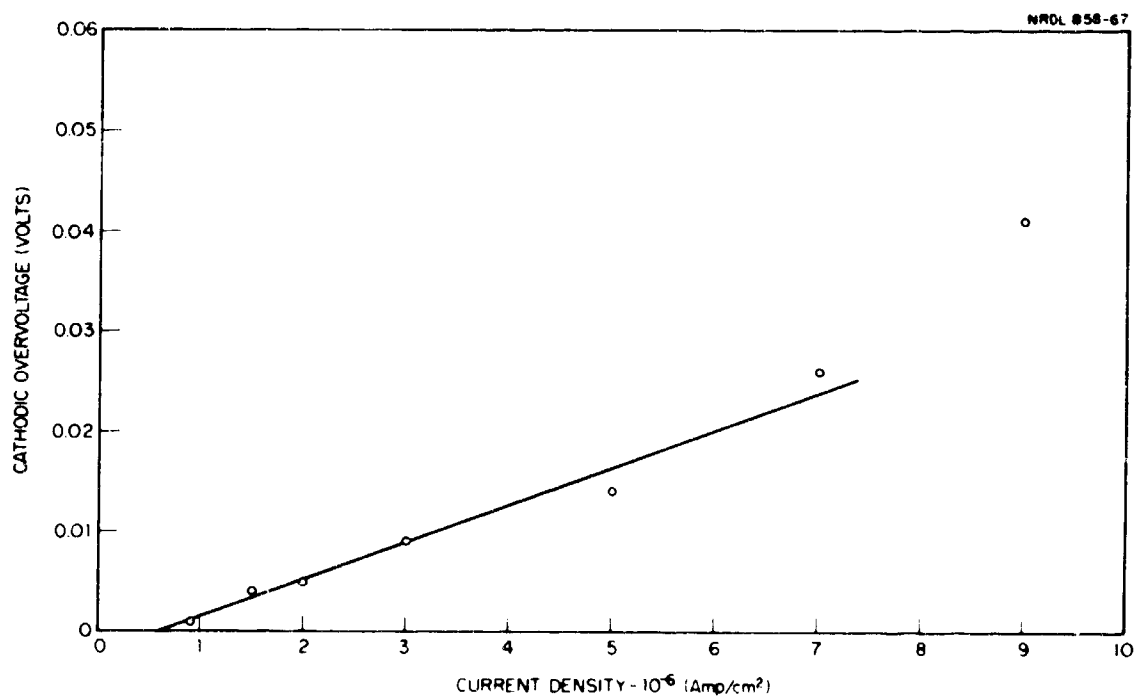


Fig. 10 Linear Plot of Cathodic Overvoltage vs. Current Density for Copper in Aerated Seawater.

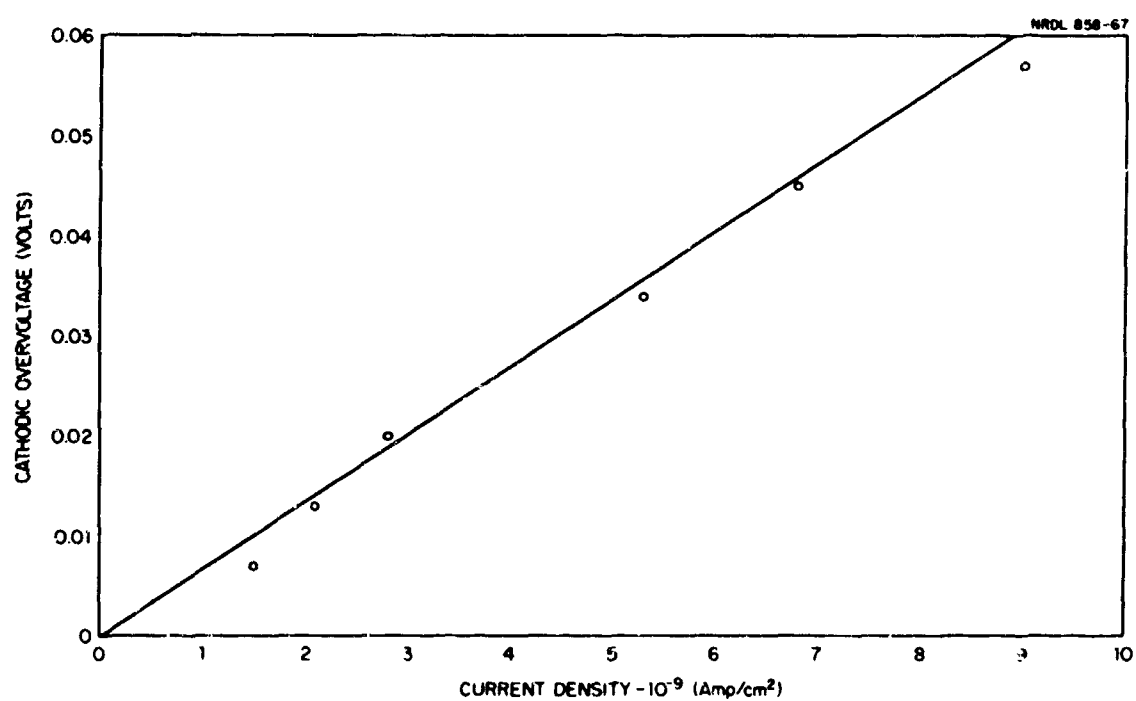


Fig. 11 Linear Plot of Cathodic Overvoltage vs. Current Density for Nickel in Deaerated Seawater.

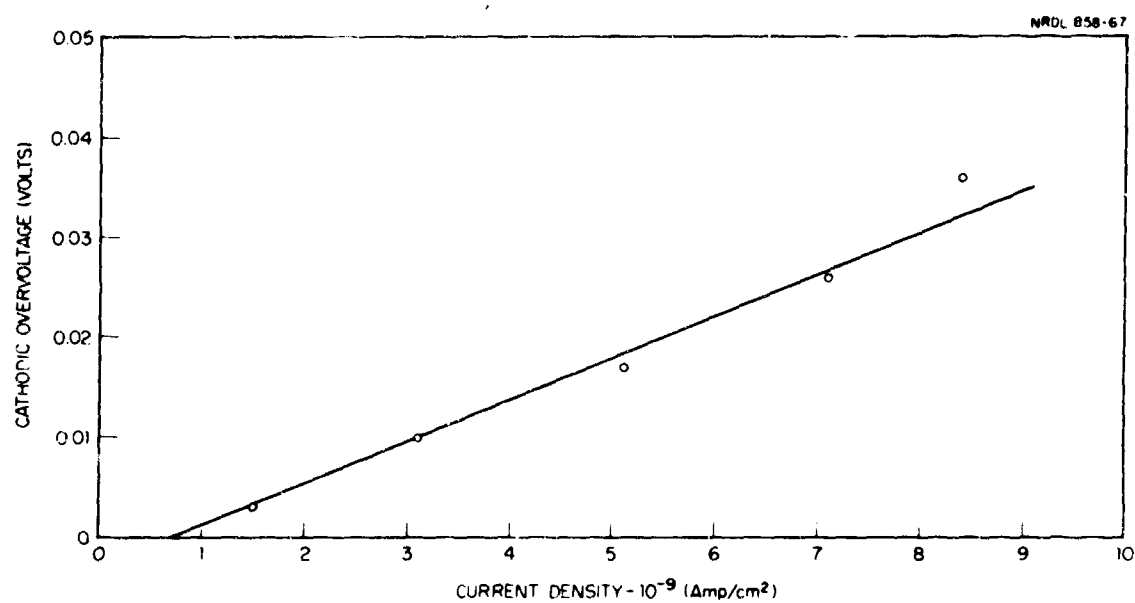


Fig. 12 Linear Plot of Cathodic Overvoltage vs. Current Density for Tantalum in Deaerated Seawater.

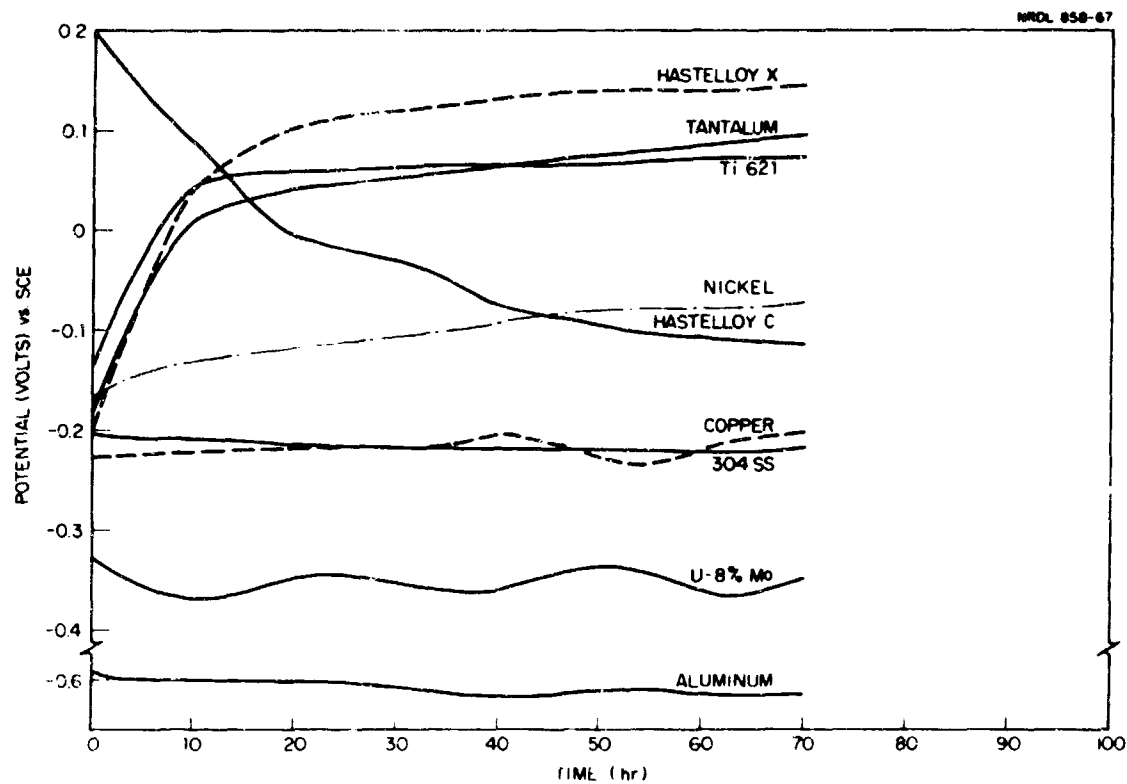


Fig. 13 Open-circuit Potentials of SNAP-21 Materials in Aerated Seawater.

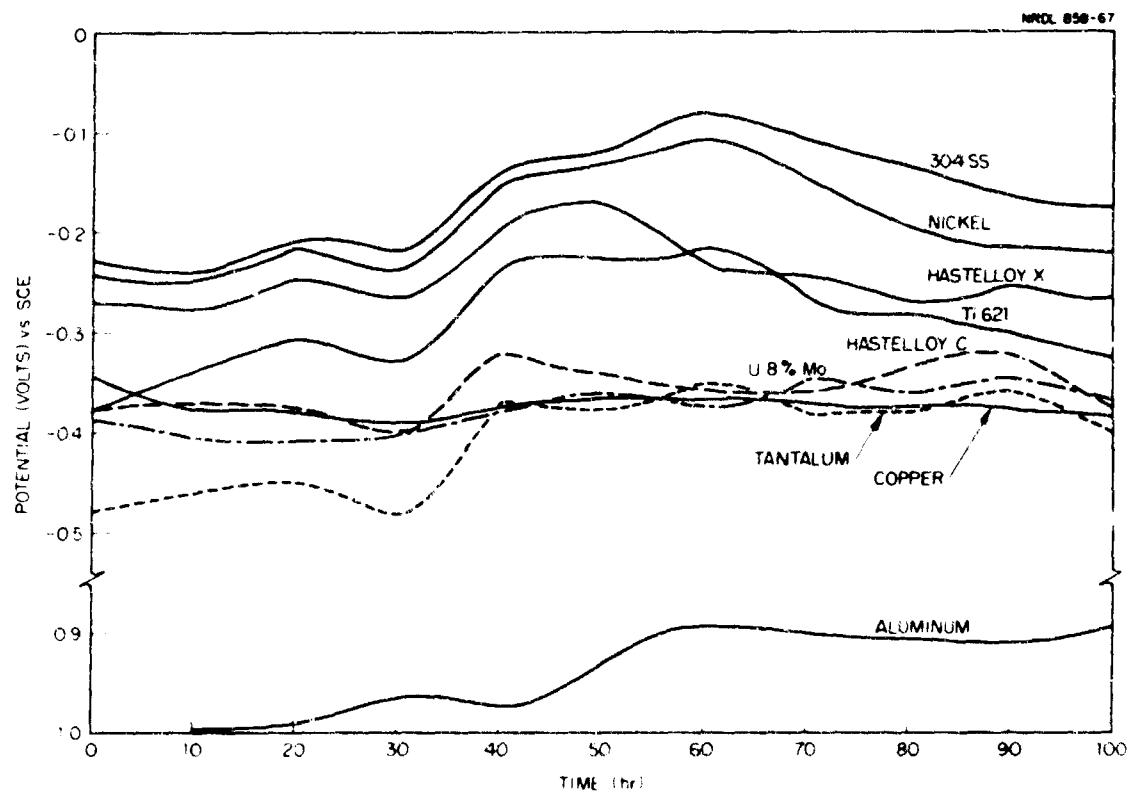


Fig. 14 Open-circuit Potentials of SNAP-21 Materials in Deaerated Seawater.

TABLE 1
Summary of Electrochemical Data From Galvanostatic Polarization of SNAP 21
Materials

Material	Seawater Condition	β_c (v)	β_a (v)	$\Delta E/\Delta i$ (v/ μ amp/cm ²)	i_{corr} (μ amp/cm ²)	Normal Corrosion Rate (mpy)
Al	Aerated	.226	.135	4.3×10^{-1}	1.1×10^{-1} (2.2×10^{-1})	4.8×10^{-2} (9.6×10^{-2})
Al*	Deaerated	.148		1.0×10^{-1}	6.3×10^{-1} (7.0×10^{-1})	2.7×10^{-1} (3.1×10^{-1})
Cu	A	.168	.072	3.6×10^{-3}	6.1 (6.2)	2.8 (2.9)
Cu	D	.376	.050	3.6×10^{-1}	5.3×10^{-2} (1.8×10^{-1})	2.4×10^{-3} (8.3×10^{-2})
Hastelloy C	A	.081	.166	2.6	9.2×10^{-3} (5.5×10^{-3})	4.4×10^{-3} (2.6×10^{-3})
Hastelloy C	D	.192	.136	3.9	9.0×10^{-3} (7.7×10^{-3})	4.3×10^{-3} (3.6×10^{-3})
Hastelloy X	A	.175	.208	2.6×10^1	1.6×10^{-3} (1.5×10^{-3})	8.0×10^{-4} (7.5×10^{-4})
Hastelloy X	D	.207	.090	6.1	4.5×10^{-3} (8.0×10^{-3})	2.3×10^{-3} (4.0×10^{-3})
Nickel	A	.076	.195	1.0×10^1	2.3×10^{-3} (1.6×10^{-3})	9.8×10^{-4} (6.8×10^{-4})
Nickel	D	.145	.175	6.8	5.1×10^{-3} (5.1×10^{-3})	2.2×10^{-3} (2.2×10^{-3})
304SS	A	.164	.220	7.9	5.2×10^{-3} (2.1×10^{-3})	2.3×10^{-3} (9.2×10^{-4})
304SS	D	.210	.163	7.9	5.1×10^{-3} (9.0×10^{-3})	2.2×10^{-3} (4.0×10^{-3})
Tantalum	A	.145	.085	7.5	3.1×10^{-3} (3.4×10^{-3})	8.7×10^{-4} (9.6×10^{-4})
Tantalum	D	.430	.137	4.2	1.1×10^{-2} (1.7×10^{-2})	3.1×10^{-3} (4.8×10^{-3})
Titanium 621	A	.145	.115	1.3×10^1	2.1×10^{-3} (2.1×10^{-3})	7.5×10^{-4} (7.5×10^{-4})
Titanium 621	D	.460	.153	4.9	1.0×10^{-2} (2.0×10^{-2})	3.6×10^{-3} (7.1×10^{-3})
U-8 % Mo	A	.359	.033	1.5×10^{-2}	8.7×10^{-1} (2.8)	3.7×10^{-1} (1.2)
U-8 % Mo	D	.390	.380	5.4×10^{-2}	1.6 (1.1)	6.8×10^{-1} (4.7×10^{-1})

*Because the anodic polarization curve for Al was very steep, the form of eq. (1) as

$$\beta_a - \beta_c \text{ was used: } \Delta E/\Delta i = \frac{\beta_c}{(2.3)i_{corr}}$$

TABLE 2
Galvanic Corrosion Currents ($\mu\text{amp}/\text{cm}^2$) of SNAP 21 Materials in Aerated Seawater

Hx	Ni	Ta	Ti 621	Hc	304ss	Cu	U-8 % Mo	Al	Σi_{cath}
2.4×10^{-1}	2.2	1.1×10^1	1.0×10^1	3.3×10^1	3.1×10^1	8.3×10^1	3.3×10^1	2.4×10^2	2.3×10^2
4.3×10^{-1}	6.0×10^{-1}	1.1×10^{-1}	1.6×10^{-1}	8.0×10^{-1}	8.7×10^{-1}	1.2×10^1	1.4×10^1		1.5×10^1
5.0×10^{-1}	5.0×10^{-1}	1.2×10^{-1}	4.7×10^{-1}	5.7×10^{-1}	5.7×10^{-1}	3.0			2.7
3.2×10^{-1}	4.0×10^{-1}	3.3×10^{-2}	1.0×10^{-1}	4.3×10^{-1}	1.3				1.3
2.5×10^{-1}	3.2×10^{-1}	2.3×10^{-2}	1.1×10^{-1}	7.0×10^{-1}					7.0×10^{-1}
2.1×10^{-3}	1.6×10^{-3}	2.2×10^{-3}	1.4×10^{-3}						3.7×10^{-3}
6.7×10^{-3}	6.7×10^{-3}								6.7×10^{-3}

TABLE 3
Galvanic Corrosion Currents ($\mu\text{amp}/\text{cm}^2$) of SNAP 21 Material in Deaerated Seawater

Hx	Ti 621	Ni	304	Ta	Hc	U-8 % Mo	Cu	Al	Σi_{cath}
2.8×10^{-1}	9.0×10^{-2}	3.1×10^{-1}	3.7×10^{-1}	6.0×10^{-2}	3.7×10^{-1}	5.0×10^{-2}	6.0×10^{-1}	2.6	2.1
2.1×10^{-3}	6.0×10^{-4}	6.0×10^{-3}	2.3×10^{-3}	2.0×10^{-4}	2.0×10^{-3}	6.0×10^{-3}	2.1×10^{-2}		1.9×10^{-2}
1.4×10^{-3}	4.0×10^{-4}	5.0×10^{-3}	1.2×10^{-3}	1.9×10^{-4}	9.0×10^{-4}	1.5×10^{-2}			1.0×10^{-2}
3.3×10^{-5}	1.3×10^{-4}	4.0×10^{-4}	4.3×10^{-5}	5.7×10^{-4}	1.7×10^{-4}				5.6×10^{-4}
2.0×10^{-5}	1.0×10^{-4}	1.3×10^{-4}							1.2×10^{-4}
3.7×10^{-4}	3.7×10^{-4}								3.7×10^{-4}

of the oxidation (metal dissolution) process. The galvanic current densities not underlined are the cathodic galvanic current densities which are a measure of the reduction processes. Theoretically, the sum of the anodic current densities must equal the sum of the cathodic current densities. Comparison of the sum of the cathodic current densities (listed in the last column of Tables 2 and 3) with the anodic current density (or sum of the anodic current densities as the case may be) of each set shows that they are in good agreement.

Note that the materials in Tables 2 and 3 are listed in a galvanic series (on the basis of the successive elimination process described above), the most noble at the left and the most active at the right. These galvanic series can be compared to those in Figs. 13 and 14 which were obtained from the measurements of open-circuit potentials. In the case of aerated seawater the order of materials is in fair agreement. In contrast, the order of materials in deaerated seawater is quite different. Apparently this is a reflection of the large variability of potential with time shown in Fig. 14. The galvanic series determined as a consequence of the galvanic current measurements is considered to be more valid since it was determined "in-situ" so to speak.

Table 4 lists the normal corrosion rate (largest value in column 7 of Table 1) and the galvanic corrosion effect (from underlined anodic galvanic currents in Tables 2 and 3) for each material in aerated and deaerated seawater. The sum of the two rates (normal and galvanic) is the total corrosion rate of the material under coupled conditions when it is the anodic member of the couple. It can be seen that in deaerated seawater the galvanic effect is small except for aluminum. For every material the galvanic effect in aerated seawater is larger. This difference in galvanic effect is due primarily to the relative differences of potentials of the materials in aerated and deaerated seawater (see Figs. 13 and 14) and to the degree of polarization. The degree of polarization is dependent on the degree of aeration. Specifically, an increase in aeration reduces cathodic polarization, thus enhancing galvanic corrosion.⁵

It must be mentioned that the galvanic effects listed in Table 4 include a surface-area effect due to the manner in which the galvanic currents were measured. This surface area effect refers to the fact that the anode-to-cathode area ratio varied for each material when it was the anode. For example, in aerated seawater the anode-to-cathode surface area ratio when aluminum was the anode was about 1 to 9; when U-8 % Mo was the anode the ratio was about 2 to 7;* when copper was the anode the ratio was 1 to 6 and so on up the galvanic series.

*The surface area of the U-8 % Mo electrode was about 2.2 times the surface areas of the other electrodes, which were equal.

TABLE 4

Normal and Galvanic Corrosion Rate of SNAP 21 Materials in Seawater

Material	Seawater Condition	Normal Corrosion Rate (mpy)	Corrosion Galvanic Effect* (mpy)
Al	A	9.6×10^{-2}	1.1×10^2
Al	D	3.1×10^{-2}	1.1
Cu	A	2.9	1.4
Cu	D	8.3×10^{-2}	9.7×10^{-2}
Hastelloy C	A	4.3×10^{-3}	3.8×10^{-1}
Hastelloy C	D	4.2×10^{-3}	8.0×10^{-5}
Hastelloy X	A	8.0×10^{-4}	
Hastelloy X	D	4.0×10^{-3}	
Nickel	A	9.8×10^{-4}	2.8×10^{-3}
Nickel	D	2.2×10^{-3}	1.6×10^{-4}
304ss	A	2.3×10^{-3}	5.7×10^{-1}
304ss	D	4.0×10^{-3}	1.9×10^{-5}
Ta	A	9.6×10^{-4}	6.2×10^{-3}
Ta	D	4.8×10^{-3}	1.6×10^{-4}
Ti 621	A	7.5×10^{-4}	5.0×10^{-4}
Ti 621	D	7.1×10^{-3}	2.0×10^{-4}
U-8 % Mo	A	1.2	7.7
U-8 % Mo	D	6.8×10^{-1}	6.4×10^{-3}

*Measured with unequal areas of anode and cathode - see text.

The effect of the surface-area ratio on galvanic currents is dependent on the polarization behavior of the anodic and cathodic members of the galvanic couple.⁵ If the anodic member of the couple polarizes (i.e., changes its open-circuit potential due to flow of the galvanic current) and the cathodic member does not, the system is under anodic control. If the reverse is true the system is under cathodic control. When both the anodic and cathodic members polarize, the system is under mixed control. For a system under anodic control an increase in the surface area of the cathode does not significantly affect the corrosion rate of the anode. For a system under cathodic control an increase in the surface area of the cathode causes a proportional increase in the corrosion rate of the anode. For a system under mixed control an increase in the surface area of the cathode causes a less than proportional increase in the corrosion rate of the anode.

Results of experiments made to determine the polarization behavior of the SNAP-21 materials when galvanically coupled are shown in Tables 5 and 6 for aerated and deaerated seawater, respectively. Emphasis should be placed on relative comparisons of the anode, cathode and coupled potentials and not on their absolute values.

The results shown in Tables 5 and 6 indicate that in aerated seawater cathodic control dominated when aluminum, U-8 % Mo and copper were anodes and anodic control dominated when the other materials were anodes; in deaerated seawater aluminum, U-8 % Mo, copper, 304ss and tantalum anodes were under mixed control and the other materials again were under anodic control.

IV. APPLICATION OF RESULTS TO THE SNAP-21 SYSTEM

An attempt to make an estimate, based on the results obtained here, of how long the radioisotopic fuel would be contained once seawater enters the interior of the system requires two basic assumptions. These are: (1) that the effective surface area (i.e., the surface area in contact with seawater) of each material is equal to its geometric surface area; (2) that all materials are in electrical and electrolytic contact with each other. Table 7 shows the geometric surface areas used for each of the materials. These surface areas were approximated from drawings furnished by 3M of the SNAP-21 system.

It was also assumed that the materials would corrode in the order shown by the galvanic series in Tables 2 and 3. Since the fuel encapsulant material, Hastelloy C, is the material of most concern, the materials more cathodic in the galvanic series will not be considered

TABLE 5

Polarization Behavior of SNAP 21 Materials in Aerated Seawater

Anode Material	Potential, Volts Vs. S.C.E.		
	Anode	Cathode	Coupled
Al	- .591	- .322	- .579
U-8%Mo	- .311	- .231	- .324
Cu	- .240	- .078	- .228
304ss	+ .085	+ .118	+ .113
Ti 621	+ .096	+ .120	+ .118
Ta	+ .102	+ .126	+ .120
Hastelloy C	+ .120	+ .129	+ .128
Ni	+ .121	+ .128*	+ .129

*This is the open-circuit potential of Hastelloy X.

TABLE 6

Polarization Behavior of SNAP 21 Materials in Deaerated Seawater

Anode Material	Potential, Volts Vs. S.C.E.		
	Anode	Cathode	Coupled
Al	- 1.049	- .331	- .599
U-8%Mo	- .412	- .292	- .355
Cu	- .318	- .095	- .284
304ss	- .121	+ .037	- .050
Ta	- .019	+ .062	+ .038
Ti 621	- .009	+ .075	+ .063
Ni	+ .063	+ .078	+ .075
Hastelloy C	+ .070	+ .083*	+ .080

*This is the open-circuit potential of Hastelloy X.

TABLE 7

Approximate Surface Areas of SNAF-21 Materials

Material	Surface Area (cm ²)
Aluminum	7×10^5
Copper	6×10^5
Hastelloy C	3×10^2
Hastelloy X	1×10^3
Nickel	4×10^5
304 Stainless Steel	1×10^4
Tantalum	1×10^3
Titanium-621	2×10^4
Uranium-8 % Mo	3×10^3

except for their surface-area effect on the corrosion rates of the materials below them.

The case of aerated seawater will be considered first.

The first material to corrode will be aluminum. The surface-area ratio of it to the rest of the materials is a little less than 1:1. This ratio, however, will quickly be reduced by corrosion of the aluminum foil insulation to about 1:500 since almost all of the surface area is due to this foil and only a very small surface area is due to the segmented ring. This anode-to-cathode ratio would increase the total corrosion rate from 1.1×10^2 to about 6×10^3 mpy since the system is under cathodic control. The segmented ring, being about 1 in. thick, would corrode away in less than a year.

The next material to start corroding is the uranium-8 % molybdenum alloy (biological shield material). The anode-to-cathode surface area ratio here is approximately 1:300. This ratio would increase its corrosion rate from 9 mpy to about 7.7×10^2 mpy since it is under cathodic control. At this corrosion rate the biological shield material, being 2.5 in. thick, would last about 3 years.

Copper, the next to corrode, has an area ratio of about 1:1 to the remaining materials, but, as in the case of aluminum, almost all of its area is due to the copper foil insulation. The anode-to-cathode area ratio would be approximately 1:700 after the insulation has corroded and only the copper cold frame is left. This ratio would increase the corrosion rate from 4.3 mpy to about 10^3 mpy. At this rate the cold frame, being 2.75 in. thick, would last about 3 years.

For the next material, 304 stainless steel, the anode-to-cathode surface area ratio (1:40) should not significantly increase its corrosion rate of 5.7×10^{-1} mpy since it is corroding under anodic control. At this rate, the 304 stainless steel liner, .125 in. thick, should last about 200 years.

The corrosion rate of the material of primary interest, Hastelloy C, should not be significantly increased since it is also under anodic control. Its corrosion rate, 3.8×10^{-1} mpy, and the thickness of the fuel container, 0.25 in., indicate the fuel would be contained for approximately 600 years.

Similar calculations can be made for the situation in which deaerated seawater is the corrosive medium. However, it can be seen from the much lower values of all the corrosion rates (Table 4) that the fuel would remain encapsulated for a much longer time in deaerated seawater.

A deaerated seawater condition could be approached in the interior of the system if the pressure vessel is breached in a manner that would cause the initial charge of seawater to become stagnant (e.g., little or no flow of fresh seawater through the interior).

Several comments can be made about the above estimates of how long the fuel would be contained. The first concerns the two basic assumptions of effective surface area and all materials' being in electrical contact with each other. In an actual situation the first assumption would not be very realistic since there are many interfaces between materials which the seawater could probably not enter. This statement is particularly true of the insulation foils of aluminum, copper and nickel. Because of these considerations the anode-to-cathode surface area ratios would be much smaller and hence the corrosion rate of the anode materials could be smaller. The second assumption that all the materials be in electrical and electrolytic contact with each other would also not be very realistic in the case of the insulating foils. They are wrapped around the uranium-8 % molybdenum biological shield in alternate layers with quartz paper between layers. This again would reduce the anode-to-cathode surface area ratios and may even eliminate a material (e.g., nickel) from the galvanic series. If the latter situation exists the corrosion rate of Hastelloy C would be smaller.

Another fact which was not taken into account in making the estimate is the effect of the accumulation of corrosion products on or near the surface of the corroding materials. This would slow down the corrosion rate.

The effect of other forms of corrosion (e.g., pitting, crevice, stress) was not considered in the above discussion. However, based on other studies, their effect on the performance of Hastelloy C is expected to be very small.^{8,9}

The above considerations show that the estimate in aerated seawater is a lower limit of how long the fuel will be contained. The relatively short half-life of the fuel, 28 years, compared to the estimate in aerated seawater, indicates that the SNAP-21 system can meet the requirement of not exposing man to the radiological hazards of the fuel. However, before a final analysis can be made, results of other studies must be considered. These studies, currently being carried out, include the effects of radiation⁶ and temperature⁷ on the corrosion behavior of the SNAP-21 system.

REFERENCES

1. D. A. Kubose and H. I. Cordova, "Electrochemical Corrosion Studies of SNAP Container Materials", U. S. Naval Radiological Defense Laboratory, USNRDL-TR-1036, 7 June 1966.
2. M. Stern and A. L. Geary, "Electrochemical Polarization. A Theoretical Analysis of the Shape of Polarization Curves", J. 104:56 (1957).
3. M. Stern, "A Method for Determining Corrosion Rates From Polarization Data", Corrosion 14:440 (1958).
4. N. D. Greene, Experimental Electrode Kinetics, Troy, New York, Rensselaer Polytechnic Institute, p. 31, 1965.
5. H. H. Uhlig, ed. The Corrosion Handbook, New York, John Wiley and Sons, Inc., p. 489, 1948.
6. L. W. Weisbecker and S. Z. Mikhail, "Basic Test Plan for Ocean Exposure Studies of SNAP-21 Radioisotope-Loaded Fuel Capsule", U. S. Naval Radiological Defense Laboratory, USNRDL-LR-67-96, 27 November 1967.
7. L. W. Weisbecker, "Basic Test Plan for Ocean Exposure Studies of SNAP-21 Electrically Heated Fuel Capsule Test Systems", U. S. Naval Radiological Defense Laboratory, USNRDL-TRC-67-15, 7 March 1967.
8. E. D. Weisert, "Hastelloy C", Chem. Eng. 59:297 (1952).
9. Compilation of Seawater Corrosion Data for Hastelloy C, Stellite Division, Union Carbide Corporation, Kokomo, Indiana, 1965.

UNCLASSIFIED

Security Classification

DOCUMENT CONTROL DATA - R & D

(Security classification of title, body of abstract and indexing annotation must be entered when the overall report is classified)

1. ORIGINATING ACTIVITY (Corporate author) U. S. Naval Radiological Defense Laboratory San Francisco, California 94135		2a. REPORT SECURITY CLASSIFICATION UNCLASSIFIED	
3. REPORT TITLE ELECTROCHEMICAL CORROSION STUDIES OF GALVANICALLY COUPLED SNAP-21 MATERIALS		2b. GROUP	
4. DESCRIPTIVE NOTES (Type of report and inclusive dates)			
5. AUTHOR(S) (First name, middle initial, last name) Donald A. Kubose Herman I. Cordova			
6. REPORT DATE APR 30 1968		7a. TOTAL NO. OF PAGES 42	7b. NO. OF REFS 9
8a. CONTRACT OR GRANT NO. AEC, DRD&T Program, AT-RDT-XP-141, Tasks b. PROJECT NO. 2a and 3b		8b. ORIGINATOR'S REPORT NUMBER(S) USNRDL-TR-68-26	
c. d.		9b. OTHER REPORT NO(S) (Any other numbers that may be assigned this report)	
10. DISTRIBUTION STATEMENT This document has been approved for public release and sale; its distribution is unlimited.			
11. SUPPLEMENTARY NOTES		12. SPONSORING MILITARY ACTIVITY Atomic Energy Commission Washington, D. C. 20545	
13. ABSTRACT Electrochemical corrosion rate measurements on materials used in the SNAP-21 radioisotopically-fueled power system have been made in seawater at room temperature. The materials examined included aluminum, copper, Hastelloy C, Hastelloy X, nickel, 3-4 stainless steel, tantalum, titanium-621 alloy and uranium-8% molybdenum alloy. The normal corrosion rate of each material was measured by means of galvanostic polarization techniques. A galvanic series of the materials in seawater was determined and the galvanic currents between galvanically coupled materials were measured with a zero-resistance ammeter circuit. The effect of galvanic coupling of construction materials of the SNAP-21 system does not materially change the containment time of the Sr-90 fuel in the corrosive seawater environment.			

DD FORM 1473 (PAGE 1)

5/N 0101-807-6801

UNCLASSIFIED
Security Classification

